
1 **The Flowering Repressor SVP recruits the TOPLESS**
2 **co-repressor to control flowering in chrysanthemum**
3 **and *Arabidopsis***

4 Zixin Zhang^{1,#,\$}, Qian Hu^{1,#}, Yuqing Zhu¹, Zheng Gao², Erlei Shang³, Gaofeng Liu¹,
5 Weixin Liu¹, Rongqian Hu¹, Xinran Chong¹, Zhiyong Guan¹, Weimin Fang¹, Sumei
6 Chen¹, Bo Sun³, Yuehui He⁴, Jiafu Jiang^{1,*}, Fadi Chen^{1,*}

7 ¹State Key Laboratory of Crop Genetics and Germplasm Enhancement, the Key laboratory of
8 Landscaping, Ministry of Agriculture, College of Horticulture, Nanjing Agricultural University,
9 Nanjing 210095, China

10 ²Shanghai Center for Plant Stress Biology, Chinese Academy of Sciences Center for Excellence in
11 Molecular Plant Sciences, Shanghai 201602, China

12 ³State Key Laboratory of Pharmaceutical Biotechnology, School of Life Sciences, Nanjing
13 University, Nanjing 210023, China

14 ⁴Peking University Institute of Advanced Agricultural Sciences, Weifang, Shandong 261000,
15 China

16 ^{\$}Current address: Key Laboratory of Bio-resource and Eco-environment of Ministry of Education,
17 College of Life Sciences, Sichuan University, Chengdu 610065, China

18

19 ***Correspondence:**

20 * Corresponding Author: Jiafu Jiang or Fadi Chen

21 College of Horticulture, Nanjing Agricultural University, Nanjing 210095, China;

22 Tel: +86-25-84399670; Fax: +86 25 84395266;

23 E-mail address: jiangjiafu@njau.edu.cn, chenfd@njau.edu.cn

24 [#]These authors contributed equally to this work.

25

26 **Abstract:** Plant flowering time is a consequence of the perception of
27 environmental and endogenous signals. The
28 MCM1-AGAMOUSDEFICIENS-SRF-box (MADS-box) gene SHORT
29 VEGETATIVE PHASE (SVP) is a pivotal repressor that negatively regulates the
30 floral transition during the vegetative phase. The transcriptional corepressor
31 TOPLESS (TPL) plays critical roles in many aspects of plant life. An interaction first
32 identified between the second LXLXLX motif (LRLGLP) of CmSVP with
33 CmTPL1-2, which can repress the expression of a key flowering factor *CmFTL3* by
34 binding its promotor CARG element in chrysanthemum. Genetic analysis suggested
35 that the CmSVP-CmTPL1-2 transcriptional complex is a prerequisite for SVP to act
36 as a floral repressor, which reduces *CmFTL3* transcriptional activity. *CmSVP* rescued
37 the phenotype of the *svp-31* mutant in *Arabidopsis*, and overexpression of *AtSVP* or
38 *CmSVP* in the *Arabidopsis* dominant negative mutation *tpl-1* led to a loss-of-function
39 in late flowering, which confirmed the highly conserved function of *SVP* in the two
40 completely different species. Thus, we have validated a conserved machinery wherein
41 SVP relies on TPL to inhibit flowering through the direct regulation of *FT*, which is
42 more meaningful for the evolution of species and could be translated to high-quality
43 cultivation and breeding of crops.

44 **Key words:** Chrysanthemum, *Arabidopsis*, flowering time, protein interaction,
45 co-repressor, *FLOWERING LOCUS T*.

46

47 **Introduction**

48 In plants, the regulation of multiple endogenous cues as well as the response to the
49 external environment is the crucial criteria for activation of flowering time (Kinoshita
50 and Richter, 2020). Sveral flowering-regulated MADS-box genes have been studied
51 in recent years, and yet poorly negative regulators are identified and understood in
52 plants. SHORT VEGETATIVE PHASE (SVP), as one transcription factor of the

53 MCM1-AGAMOUSDEFICIENS-SRF (MADS)-box gene family, can respond to
54 themosensory, gibberellin, and autonomous pathways (Andrés et al., 2014; Fernández
55 et al., 2016). An analyses of evolution showed that the SVP are highly conserved and
56 present in nearly all eudicot species (Liu et al., 2018).

57 Mutants of *SVP* show a phenotype of early flowering under long days (LDs) or short
58 days (SDs) that represses the expression of *FLOWERING LOCUS T (FT)*, *TWIN*
59 *SISTER OF FT (TSF)*, and *SUPPRESSOR OF OVEREXPRESSION OF CONSTANS1*
60 (*SOCI*) to maintain the vegetative phase of plants (Andrés et al., 2014; Hartmann et
61 al., 2000; Jang et al., 2009; Li et al., 2008). The study of *Arabidopsis* indicated that
62 SVP could bind to the CC (A/T)₆ GG (CArG) in the promoter region and form a
63 dimer complex to play a regulatory function (Folter and Angenent, 2006; Gregis et al.,
64 2013; Hartmann et al., 2010), but the negative action controlled by this
65 MADS-domain transcription factor is unclear.

66 And yet a transcriptional co-repressor TOPLESS (TPL)/TPL-RELATED (TPR) is also
67 involved in a set of proteins responsible the switch from vegetative to reproductive
68 phase by inhibiting transcription of *FT* (Causier et al., 2012; Goralogia et al., 2017;
69 Krogan et al., 2012; Zhang et al., 2019). TPL/TPR family proteins, as universal
70 transcription GRO/Tup1-like co-repressors, are widely present in plants and
71 participate in the biological processes of growth and development, such as plant
72 hormone signaling pathways, various stress responses, and cycle rhythm clock
73 regulation (Causier et al., 2012; Plant et al., 2021). TPL/TPR protein is able to interact
74 with specific transcription factors directly or indirectly, thereby inhibiting the
75 expression of target genes and the performance of the signal transduction pathway
76 (Pauwels et al., 2010). The mutation (*tpl-1*) at the 176th amino acid position of the
77 N-terminal domain of the TPL protein from aspartic acid to histidine is a dominant
78 negative mutation that can cause dramatic temperature-sensitive abnormalities in
79 growth and development, and TPL has been confirmed as a transcriptional
80 co-repressor that interacts with the EAR domain of IAA12/BDL to control *ARF*

81 transcriptional activity in an auxin-dependent manner (Long et al., 2006). Studies
82 have suggested that TPL/TPR genes have a function during the transition to
83 flowering (Leydon et al., 2021). Barry (Causier et al., 2012) found that the delayed
84 flowering caused by TOE1's inhibition of *FT* expression is dependent on TPL/TPR.
85 TPL can interact with CO through the microprotein miP1a/b, thereby inhibiting the
86 expression of *FT* and delaying the flowering of *Arabidopsis* (Graeff et al., 2016).
87 Further research has revealed the function of the microprotein miP1a in floral
88 repression, in which a repressor complex with miP1a/b, CO/CO-like transcription
89 factors, TPL, and JM14 prevents flowering by repressed *FT* gene transcription in
90 *Arabidopsis* (Rodrigues et al., 2021). The dominant negative *tpl-1* mutant sequence is
91 driven by the endogenous gene *SUC2* promoter, which results in the flowering time
92 being significantly earlier in *Arabidopsis*. The study further speculated that
93 CYCLING DOF FACTOR 1 is combined with TPL to regulate the expression of *CO*
94 and *FT*, thus, inhibiting flowering in the photoperiod pathway (Goralogia et al., 2017).
95 A recent study found that GA signals could be mediated by the GAF1-TPR complex
96 to repress the expression of *ELF3*, *SVP*, and TEMs, which leads to the induction of
97 *FT* and *SOC1* (Fukazawa et al., 2021).

98 Chrysanthemum is one of the most important ornamental plants used worldwide, and
99 it is widely cultivated as cut, potted, and garden flowers, and the flowers of some
100 cultivars are a resource for medicinal materials (Teixeira, 2003). Therefore, the
101 ornamental and commercial values are dependent on the appropriate time of year. And
102 the discovery of key genes involved in the vegetative stage and responses to
103 temperature or light have great significance for generating new chrysanthemum
104 cultivars and ensuring year-round production. In previous studies, *Arabidopsis FT*
105 homologous genes *CsFTL1*, *CsFTL2*, and *CsFTL3* were cloned from *Chrysanthemum*
106 *seticuspe* and *CsFTL3* was further elucidated as a key factor in the photoperiod
107 pathway of chrysanthemums (Oda et al., 2012). The CONSTANS homologous gene
108 *CmBBX8* belonging to the BBX family isolated from a day-neutral chrysanthemum

109 ‘Yuuka’ accelerates flowering by targeting *CmFTL1* directly (Wang et al., 2020).
110 Another member of the BBX family in chrysanthemums, *CmBBX24* suppresses
111 flowering time by inhibiting GA biosynthesis (Yang et al., 2014). The *TERMINAL*
112 *FLOWER 1* homologous gene *CsAFT* can inhibit flowering through the disruption of
113 the FT-FD complex (Higuchi et al., 2013). *CmNF-YB8* is involved in the age pathway
114 to accelerate the transition from the juvenile to adult phase in chrysanthemums (Wei
115 , Y. et al., 2017). We previously identified a highly homologous gene to *SVP* in the
116 chrysanthemum ‘QD026’, which we named *SVPI* (CL11972. Contig2_All), and its
117 expression level declined while that of *FT* increased based on a result of RNA-seq
118 during floral transition (Cheng et al., 2018). In the present study, *CmSVP* was cloned
119 from the chrysanthemum ‘Jinba’ and the transgenic chrysanthemum was generated.
120 The expression of *CmFTL3* was detected, respectively, in overexpression and
121 knockdown lines of *CmSVP*, which suggests that the expression pattern of *CmFTL3* is
122 negatively regulated by *CmSVP*. Evidence from the genetic and ChIP assay showed
123 that *CmSVP* is responsible for the reduction in *CmFTL3* transcription directly. Then,
124 we showed that *CmSVP* recruits *CmTPL1-2* to reduce *CmFTL3* transcription in the
125 chrysanthemum ‘Jinba’, and the mechanism is also conservative in *Arabidopsis*. The
126 combined data reveal that *SVP* repressing flowering to keep the plants in a vegetative
127 stage depends on *TPL* activity. As *Arabidopsis* is a facultative long-day plant, and
128 chrysanthemum ‘Jinba’ is a strict short-day variety that takes on a complex hexaploid,
129 a highly conserved *SVP-TPL* machinery is significance for the species evolution. And
130 moreover, These findings will help to elucidate the functions of numerous orthologous
131 and homologous genes in floral transition in plants.

132

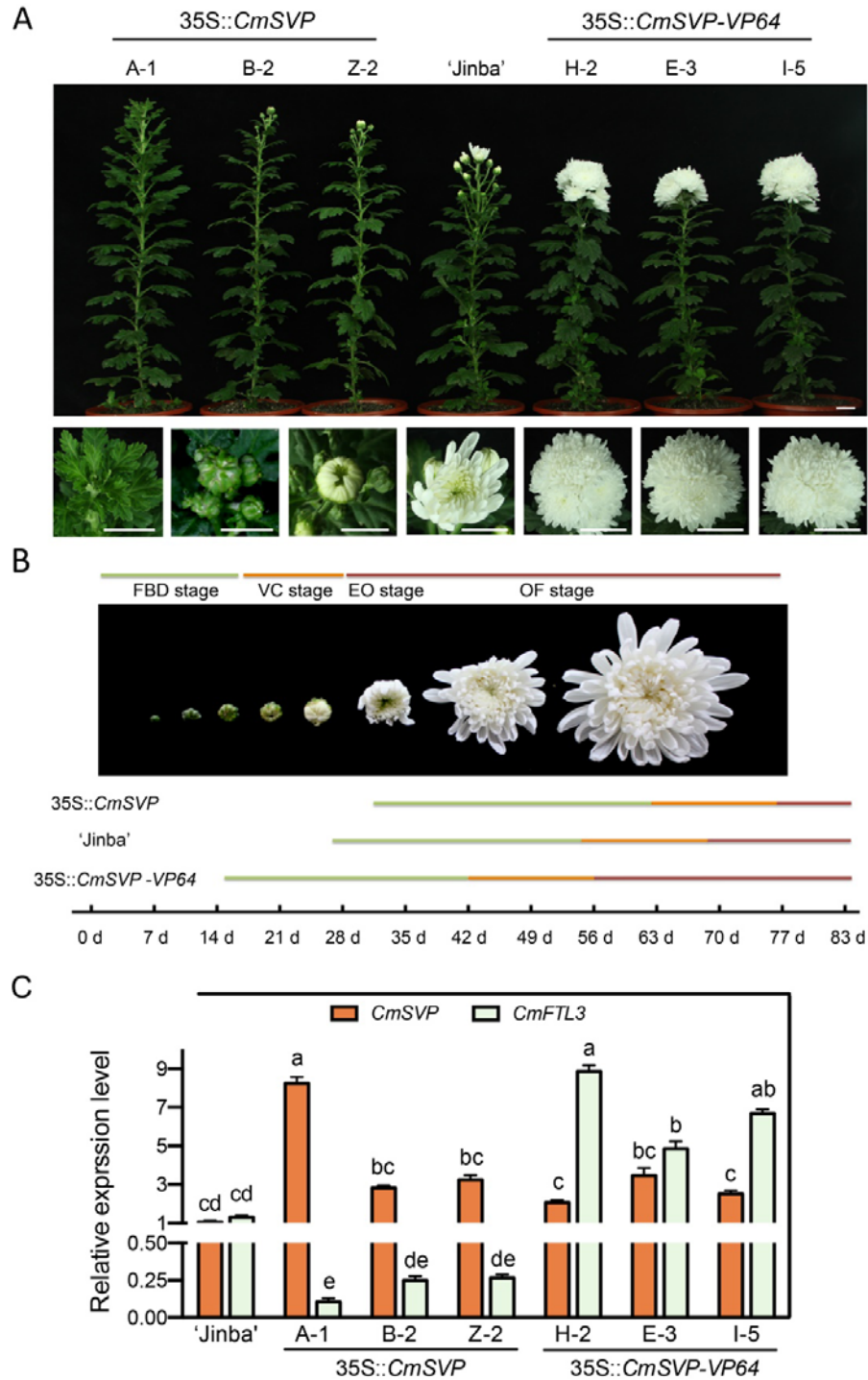
133 **Results**

134 ***CmSVP* delays the transition to flowering in chrysanthemum**

135 To determine the function of *CmSVP* in the chrysanthemum ‘Jinba’, the length of
136 *CmSVP*, which was cloned from ‘Jinba’, consists of a 669 bp coding sequence and
137 encodes 223 amino acids with a predicted molecular mass of 25.46 kDa and a *pI*
138 (isoelectric point) of 6.797. The sequence features and expression pattern of *CmSVP*
139 in chrysanthemums were initially verified (Fig. S1). The sequence features a
140 conserved MADS domains at the N termini, which contain the non-translatable
141 binding site of miR396 (Fig. S1A). As the *SVP* mRNA in *Arabidopsis* decays, it is
142 triggered by miR396(Palatnik et al., 2003; Yang et al., 2015). *CmSVP*-mut396 with
143 four mismatches in the core pairwise region of miR396 was obtained by site-directed
144 mutagenesis to avoid the miR396-mediated translation inhibition (Fig. S1A). As
145 tested by the yeast hybrid system, *CmSVP* is not related to any of the transcriptional
146 autoactivation activities, while the VP16 is a fragment of viral DNA sequence that can
147 reverse the feature (Fig. S1B). Evolutionary analysis showed that *CmSVP* is closely
148 related to AaSVP, which is derived from *Artemisia annua* (Fig. S1C, Fig. S2).
149 Moreover, the specific sequence information is shown in Fig. S2. The relatively high
150 abundance of the transcript was present in stems of the vegetative phase, followed by
151 the leaves and buds at the reproductive stage (Fig. S1D). In addition, laser confocal
152 microscopy was employed to reveal the GFP signals of *CmSVP*-GFP fusion gathered
153 in the nuclei, while those of control 35S::GFP were presented in the whole cell (Fig.
154 S1E).

155 In the chrysanthemum ‘Jinba’, a strategy that involves the recruitment of
156 additional VP64 for 35S::*CmSVP*-VP64 fusion was used to reverse its transcriptional
157 repressor activity. VP64 is the four tandem repeats of VP16, which is capable of
158 turning a repressive transcription regulator into an activator completely. And may
159 causes a similar or stronger phenotype compared to the knockout plants(Guo et al.,
160 2018; Suzuki et al., 2014; Triezenberg et al., 1988). Three transgenic lines (H-2, E-3,

161 and I-5) of 35S::*CmSVP-VP64* were selected that flowered significantly earlier than
162 the wild type (WT) plant ‘Jinba’, while 35S::*CmSVP* (OX) (A-1, B-2, and Z-2)
163 showed a later flowering time compared to WT ‘Jinba’ (Fig. 1A, B, Fig. S3) with
164 molecular identification (Fig. S4A, Fig. 1C). The first involucre primordia was
165 initiated in 35S::*CmSVP-VP64* plants, 14 days after being transplanted and grown
166 under SD conditions. This developmental stage was 13 days earlier than in WT plants.
167 When the 35S::*CmSVP-VP64* plants had already reached the open-flower stage, the
168 OX plants were still at the bud formation stage, which was 20–23 days later than that
169 in WT plants (Fig. 1B). We next investigated whether the expression of *CmFTL3*
170 changed in transgenic plants. Compared to the WT ‘Jinba’, 35S::*CmSVP* plants
171 showed dramatically decreased levels of *CmFTL3* mRNA, while 35S::*CmSVP-VP64*
172 plants presented an increasing trend (Fig. 1C).



173

174 **Fig. 1 Phenotypes of *CmSVP* transgenic 'Jinba' plants**

175 A. The phenotypic consequence of overexpression (A-1, B-2, and Z-2) and a
 176 constitutively active form of *CmSVP* (H-2, E-3, and I-5). Scale bar = 1.5 cm.

177 B. Developmental process of flower buds in wild type 'Jinba' and transgenic plants.

178 Flowering time was calculated after being transplanted and grown under SD
179 conditions. FBD, represents the flower bud development stage, VC represents the
180 visible color stage, EO represents the earlier opening stage, and OF represents the
181 open-flower stage.

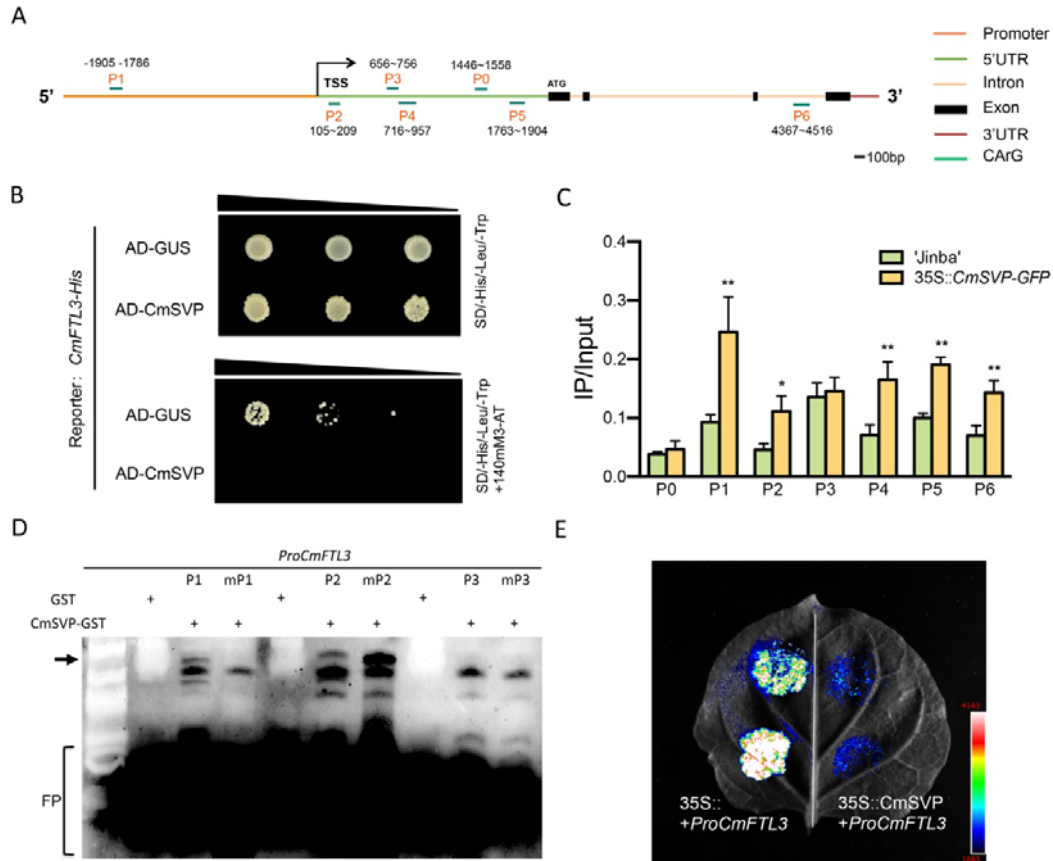
182 C. Transcript level of *CmSVP* and *CmFTL3*, respectively, in 35S::*CmSVP* and
183 VP64-*CmTPL1-2* transgenic chrysanthemums as well as wild type ‘Jinba’. Data
184 represent the mean \pm SEM of biological triplicates. Different letters represent a
185 significant difference at $P < 0.05$ (one-way ANOVA with Fisher’s post hoc test).

186

187 **CmSVP inhibits the transcription of *CmFTL3* by binding its promoter**

188 To investigate whether CmSVP is capable of regulating the transcription of *CmFTL3*
189 directly, we performed yeast one-hybrid (Y1H) assay. First, seven CArG elements of
190 the *CmFTL3* genome sequence were selected as possible binding sites (P0-P6) (Fig.
191 2A). The results of Y1H showed that CmSVP could bind the full-length promoter of
192 *CmFTL3* (Fig. 2B); then, the promoter was further segmented to confirm the
193 interaction, which showed that CmSVP could interact with P1, P2, and P4 fragments,
194 while P0, P3, P5, and P6 were the non-binding ones (Fig. S5). To further examine the
195 CmSVP binding region of the *CmFTL3* genome sequence, ChIP-qPCR was used to
196 screen the binding elements enriched by CmSVP. we found that CmSVP was able to
197 target the CArG element in the promoter, 5’UTR, and intron regions. P0 and P3 are
198 invalid sites for CmSVP binding, which is consistent with the results found in yeast
199 (Fig. 2C, Fig. S5). As shown in Fig. S6, we detected the GFP-tag in the GFP fusion
200 expression target protein CmSVP for ensuring the reliability of the assay. The EMSA
201 assay with normal and mutation probes with the CArG motif in the promoter (P1 and
202 mP1) and 5’UTR (P2, mP2; P3, and mP3) of *CmFTL3* suggested that CmSVP was
203 also able to bind the *CmFTL3* promoter in vitro (Fig. 2D). The fragment of the
204 sequence is shown in Fig. S7. The dual luciferase reporter assays by using
205 35S::*CmSVP* as an effector and *ProCmFTL3* as a reporter showed that the

206 co-expression of the effector and reporter constructs reduced the *ProCmFTL3* activity
 207 effectively compared to the control groups (Fig. 2E). These results indicated that
 208 CmSVP could recognize and regulate *CmFTL3* directly in chrysanthemums.



209

210 **Fig. 2 CmSVP directly binds to the CArG motif in the promoters of *CmFTL3***

211 A. Schematic diagrams showing the *CmFTL3* genomic regions. The promoter is
 212 represented by an orange line, 5'UTR is represented by a green line, introns are
 213 represented by a light orange line, while exons are represented by black boxes. A
 214 flat ellipse (P0-P6) indicates the sites that have either single mismatch or are
 215 perfectly matched to the consensus binding sequence (CArG box) of MADS
 216 domain proteins. TSS, transcription start site.

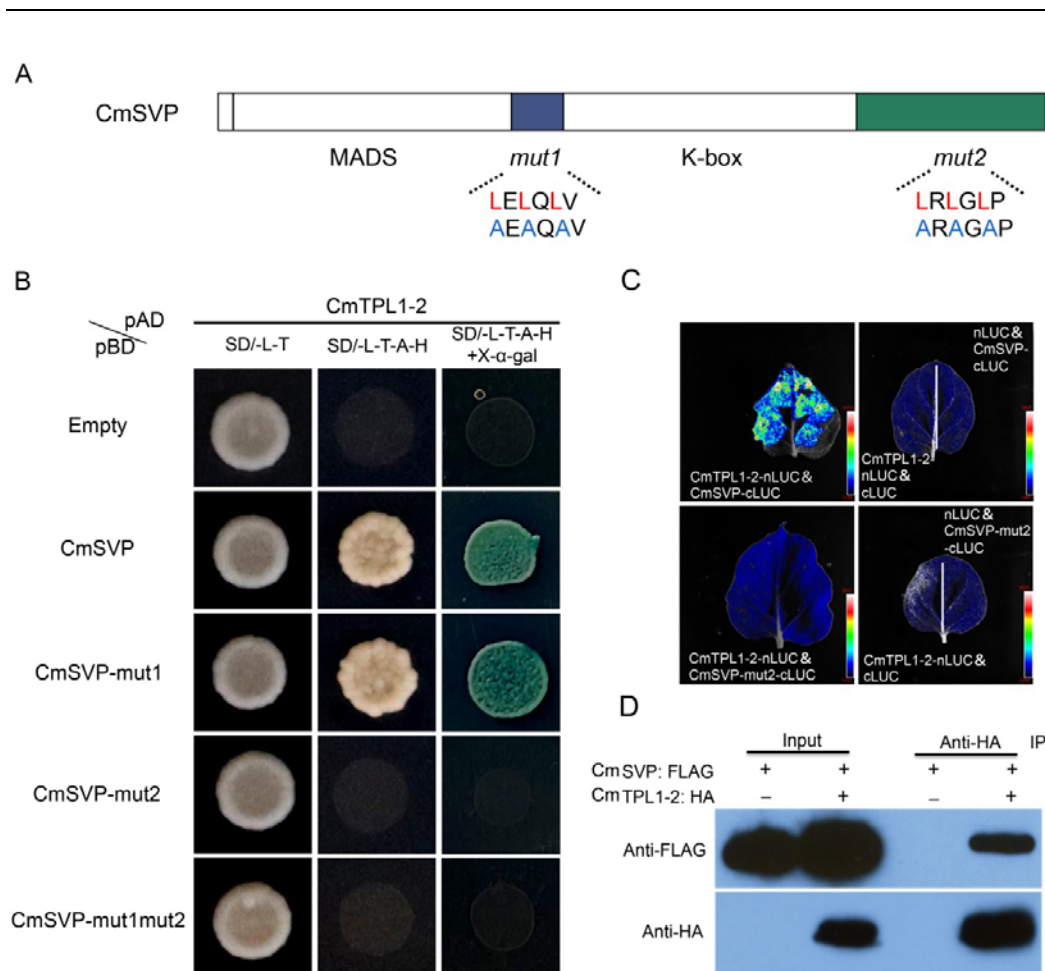
217 B. Interactions between CmSVP proteins and the promoters of *CmFTL3* in yeast
 218 cells. The 2249 bp fragment cloned in the promoter. pGADT7-GUS was used as a
 219 negative control. SD/-His/-Leu/-Trp indicates His, Leu, and Trp synthetic dropout
 220 media. 3-AT concentrations: 140 mM for *ProCmFTL3*.

-
- 221 C. ChIP analysis of CmSVP binding to the regions of *CmFTL3* in the wild type
222 ‘Jinba’ and transgenic lines of 35S::*CmSVP-GFP* chrysanthemums. Error bars
223 indicate S.D. (n = 3 biological replicates). *P < 0.05 (Student’s *t*-test) for
224 transgenic plants versus ‘Jinba’.
- 225 D. EMSA of CmSVP binding to the P1/mP1, P2/mP2, and P3/mP3 fragment. ‘P1, P2,
226 and P3 indicate labeled DNA probes, while mP1, mP2, and mP3 indicate mutated
227 probes. Sequences are shown in Fig. S7. ‘+’ indicates presence and ‘-’ indicates
228 absence. FP, free probe.
- 229 E. Interactions of CmSVP proteins and the promoters of *CmFTL3* confirmed with
230 dual luciferase reporter assays. The obtained sequence fragment of 2249 bp and
231 P1 in *CmFTL3* promoter were detected as presented. 35S::*ProCmFTL3* and
232 35S::*ProCmFTL3-P1* were used as controls.

233

234 **The interaction between CmSVP and CmTPL1-2**

235 To elucidate the mechanism of CmSVP as a negative flowering regulator, a yeast
236 two-hybrid (Y2H) assay was performed. With CmSVP as the bait protein, a cDNA
237 fragment showing homology to the *Arabidopsis* TPL was identified, which was
238 designated CmTPL1-2. Its characteristics were reported in our previous study (Zhang
239 et al., 2019). CmSVP could interact with CmTPL1-2 in the yeast assay in vitro (Fig.
240 3A). CmSVP contains two EAR domains (LXLXLP), and we further confirmed that
241 the interaction site of CmSVP-CmTPL1-2 occurred at the second EAR domain
242 (LRLGLP) of the CmSVP (Fig. 3B). Moreover, firefly luciferase complementation
243 imaging and co-immunoprecipitation (CO-IP) assay verified the interaction (Fig. 3C,
244 D). Interestingly, the interaction between AtSVP and AtTPL in *Arabidopsis* was also
245 confirmed in vitro and in vivo (Fig. S8), which indicated that the functions of SVP
246 and TPL may be conserved in chrysanthemums and *Arabidopsis*.



247

248 **Fig. 3 CmSVP interacts with CmTPL1-2**

249 A. Schematic representation of the structure of CmSVP and highlighting the mutation
250 of the two LXLXLX domains.

251 B. The interactions were tested by yeast-two-hybrid. The yeast was transformed with
252 empty vector or fusions of CmSVP, CmSVP-mut1, CmSVP-mut2, and
253 CmSVP-mut1mut2 to the Gal4-binding domain (pBD), and fusions of CmTPL1-2
254 to the Gal4 activation domain (pAD). The yeast growth on nonselective (-L-T)
255 and selective (-L-T-A-H without or with X- α -gal) SD medium. The second EAR
256 motif LRLGLP was a determinant of the interaction between CmSVP and
257 CmTPL1-2.

258 C. FLuCI assay. Quantitative analysis of luminescence intensity showing the
259 interaction between CmSVP and CmTPL1-2 in *N. benthamiana* epidermal cells.
260 CmSVP/CmSVP-mut2 were fused to the C-terminal fragment of luciferase

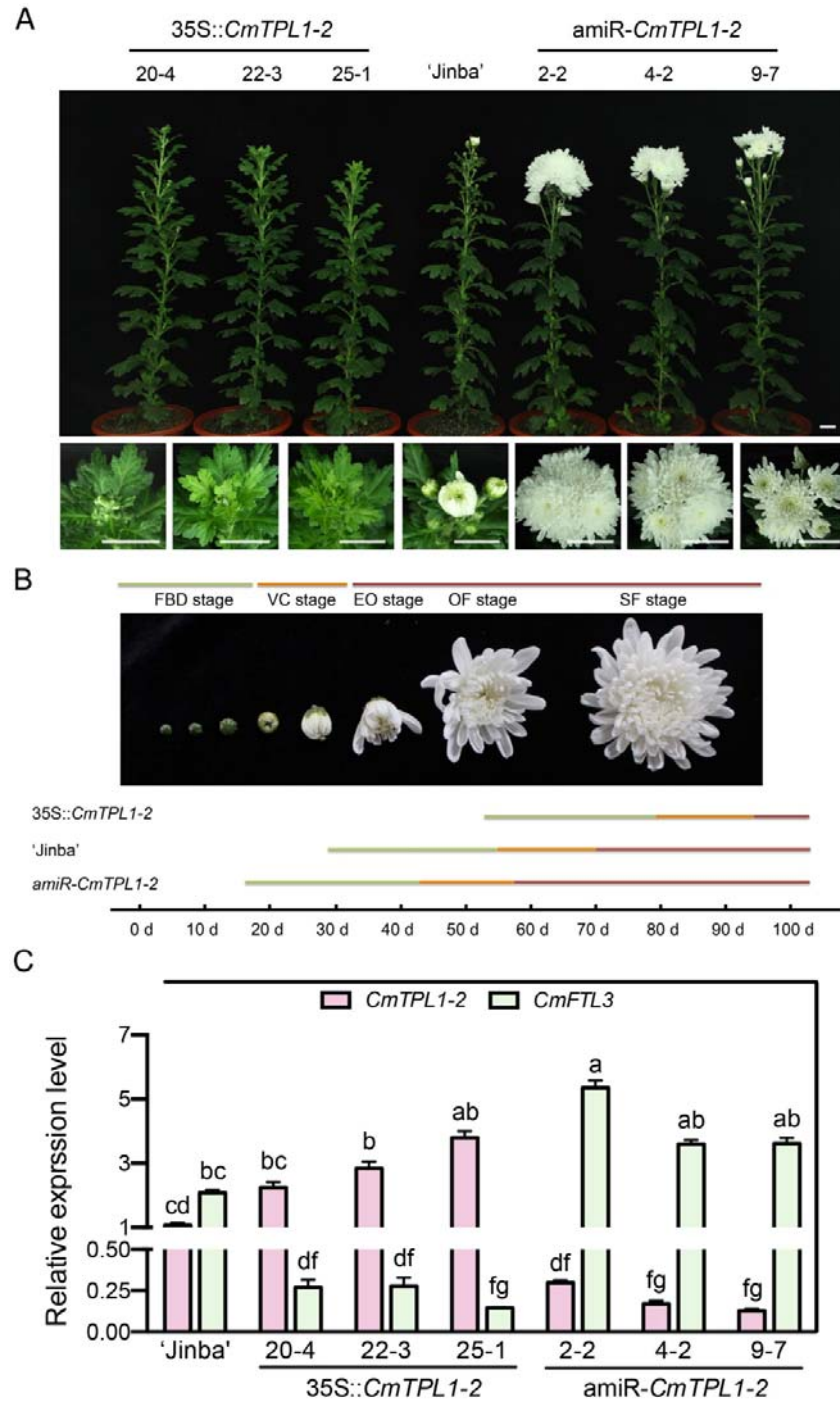
261 (cLUC), while CmTPL1-2 was fused to the N-terminal fragment of luciferase
262 (nLUC). The interactions between nLUC and CmSVP/CmSVP-mut2-cLUC as
263 well as CmTPL1-2-nLUC and cLUC were used as negative controls.
264 Representative images of *N. benthamiana* leaves 72 h after infiltration are shown.
265 D. Co-IP assay. CmTPL1-2-HA was pulled-down by immunoprecipitation of
266 FLAG-tagged CmSVP. *N. benthamiana* leaves were agroinfiltrated with
267 CmSVP-FLAG and CmTPL1-2-HA. Two days after agroinfiltration, total protein
268 extracts were immunoprecipitated with an anti-FLAG antibody. CmTPL1-2-HA
269 was detected in these fractions with an anti-HA antibody.

270

271 ***CmTPL1-2* suppresses flowering time in chrysanthemums**

272 In our previous study, the *TPL1-2* overexpression transgenics produced a higher
273 number of rosette leaves and flowered around 15 days later than Col-0 (Zhang et al.,
274 2019). The N176H mutation in the TPL of *Arabidopsis* is necessary and sufficient to
275 induce the *tpl-1* mutant phenotype (Long et al., 2006; Szemenyei et al., 2008). We
276 found that *hsp::mutCmTPL1-2* (N176H) lines would fail in floral repression when the
277 176th amino acid of CmTPL1-2 was mutated from aspartic to histidine, which
278 correlated with the late flowering phenotype compared to the Col-0 of *Arabidopsis*
279 plants (Zhang et al., 2019). To further confirm the function of *CmTPL1-2* in
280 chrysanthemums, each of three transgenic chrysanthemums, *amiR-CmTPL1-2*, and
281 *OX-CmTPL1-2* (*35S::CmTPL1-2*) lines were selected after molecular identification
282 (Fig. S8). Each of three independent overexpression lines (20-4, 22-3, and 25-1)
283 flowered later than ‘Jinba’, while the *amiR-CmTPL1-2* (2-2, 4-2, and 9-7) and
284 *hsp::mut-CmTPL1-2* (3-8, 4-2A, and 7-3) lines flowered significantly earlier than
285 ‘Jinba’ (Fig. 4A, Fig. S9). At 15 days after transplantation and being grown under SD
286 conditions, *amiR-CmTPL1-2* plants were already exhibiting differentiation of the
287 involucreal primordia, which took place 12–15 days earlier than the WT plants.
288 Moreover, the *amiR-CmTPL1-2* plants that had already reached the VC represented

289 the visible color stage, while the OX plants were still 10–13 days away from the
290 flower buds emerging phase, which was 22–25 days later than that in the WT plants
291 (Fig. 4B). We then investigated whether the expression of *CmFTL3* was changed in
292 *CmTPL1-2* transgenic chrysanthemums. We found that the levels of *CmFTL3* mRNA
293 in 35S::*CmTPL1-2* plants showed a dramatic decrease, but exhibited an increase in
294 amiR-*CmTPL1-2* plants compared with the WT ‘Jinba’ (Fig. 4C). These results
295 confirmed the interaction between CmTPL1-2 and CmSVP genetically.



296

297

298 **Fig. 4 Phenotypes of *CmTPL1-2* transgenic 'Jinba' plants**

299 A. The phenotypic consequence of overexpression (20-4, 22-3, and 25-1) and
 300 knocking down (2-2, 4-3, and 9-7) of *CmTPL1-2*. Scale bar = 1.5 cm.

301 B. Developmental process of flower buds in wild type 'Jinba' and transgenic plants.

302 Flowering time was calculated after being transplanted and grown under SD
303 conditions. FBD represents the flower bud development stage, VC represents the
304 visible color stage, EO represents the earlier opening stage, and OF represents the
305 open-flower stage.

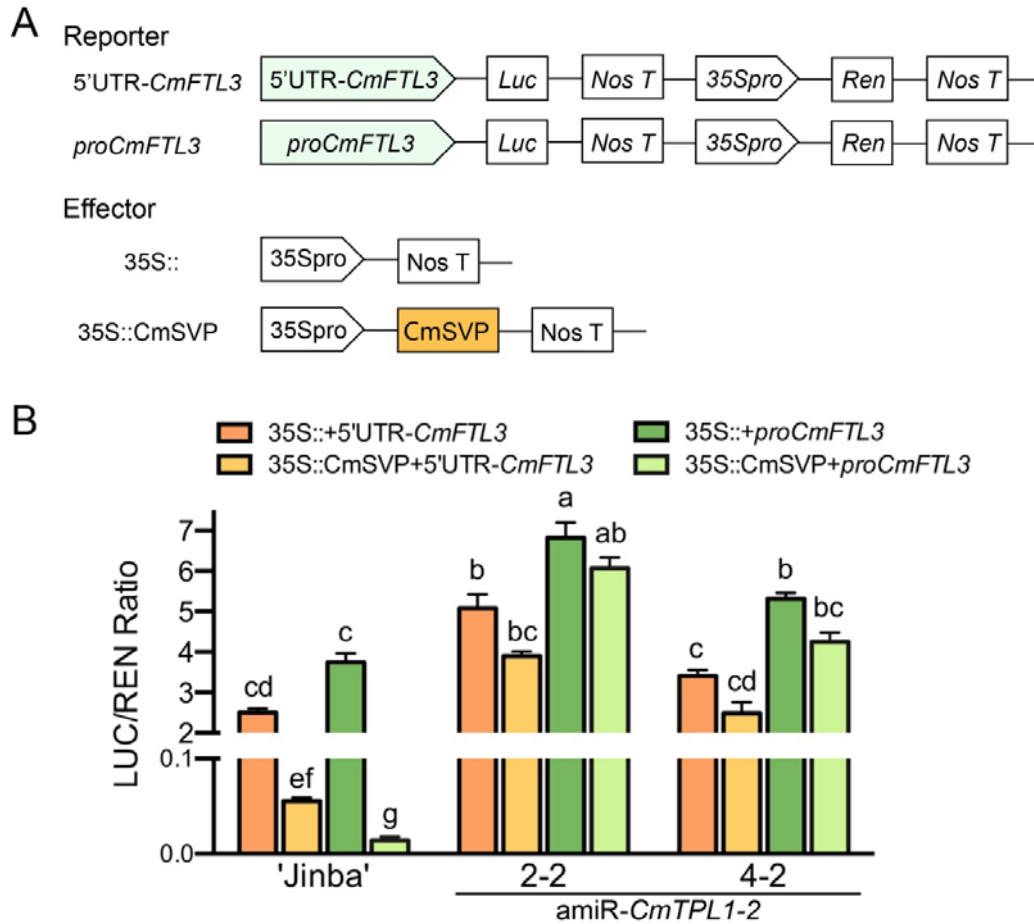
306 C. The transcript level of *CmTPL1-2* and *CmFTL3*, respectively, in 35S::*CmTPL1-2*
307 and amiR-*CmTPL1-2* transgenic chrysanthemums. Data represent the mean \pm SEM of
308 biological triplicates. Different letters represent a significant difference at $P < 0.05$
309 (one-way ANOVA with Fisher's post hoc test).

310

311 **CmSVP recruits CmTPL/CmTPR to repress CmFTL3 in the floral transition of** 312 **chrysanthemums**

313 Because the TPL functions as a co-repressor, it is suggested that the transcription
314 repression level regulates *CmFTL3* by *CmSVP* requiring *CmTPL1-2*. To investigate
315 this, a reporter and effector vector construction was used for a transient assay in
316 chrysanthemum protoplasts. The sequence of 5'UTR and the promoter of *CmFTL3*
317 was fused with the *LUC* reporter gene, respectively (Fig. 5A). The 5'UTR-*CmFTL3*
318 and *proCmFTL3* were strongly repressed by CmSVP in 'Jinba', and CmSVP
319 presented stronger repression activity in the *CmFTL3* promoter compared with 5'UTR.
320 Therefore, the protoplast isolated from amiR-*CmTPL1-2* transgenic chrysanthemum
321 was used for transcription activity detection. Moreover, the activity was partly
322 repressed, which may be due to the incomplete disappearance of CmTPL1-2 and the
323 existing homologous genes of CmTPL/CmTPR (Fig. 5B). Therefore, the obtained
324 mutation of *CmTPL1-2* (N176H) refers to mut*CmTPL1-2*, which was present in
325 loss-of-function of all CmTPL/CmTPR family members, and was used for
326 transcription activity detection. The results showed that 5'UTR and the promoter of
327 *CmFTL3* remained rarely changed in mut*CmTPL1-2* with a heat shock vector
328 (pMDC30) transgenic 3-8 line compared to the WT 'Jinba' after 37°C treatment (Fig.
329 S10). The results suggested that the CmSVP-dependent repression of *CmFTL3* in the

330 loss of CmTPL/CmTPR function in chrysanthemums was impaired.



331

332 **Fig. 5 CmSVP suppresses *CmFTL3* transcription mediated by CmTPL/CmTPR activity**

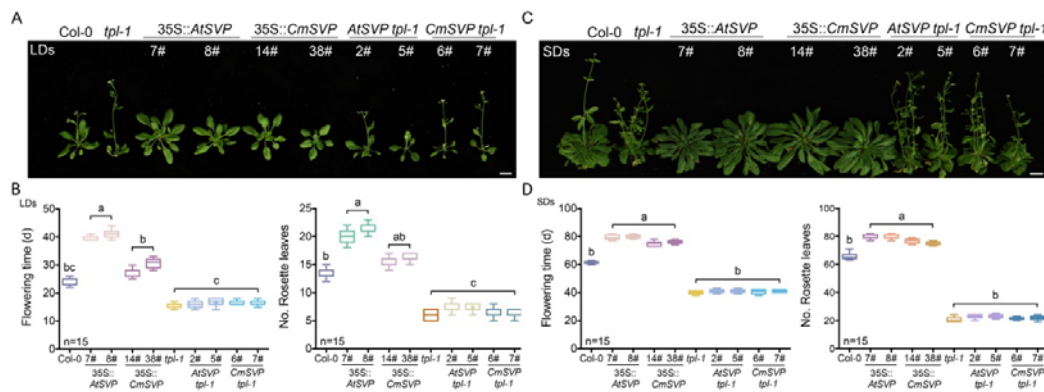
333 A. The construction diagram of the reporter 5'UTR-*CmFTL3* and *proCmFTL3* and
334 effectors.

335 B. Transient expression analysis in protoplasts of chrysanthemum genetic
336 transformation lines (*amiR-CmTPL1-2*). Repression of *CmFTL3* by CmSVP was
337 mostly dependent on CmTPL1-2. The LUC/REN is the average ratio of the
338 bioluminescence of firefly luciferase to that of firefly luciferase. Data represent
339 the mean \pm SEM of biological triplicates. Different letters represent a significant
340 difference at $P < 0.05$ (one-way ANOVA with Fisher's post hoc test).

341

342 **Dependence of SVP relies on TPL/TPR in the regulation of flowering is conserved**
343 **in chrysanthemum and *Arabidopsis***

344 To determine the conserved function of SVP recruiting for TPL to suppress its target
345 gene expression, we further performed the related assay in *Arabidopsis* mutant *tpl-1*,
346 which acts as a type of dominant negative allele for multiple TPL/TPR family
347 members. 35S::*AtSVP* *tpl-1* and 35S::*CmSVP* *tpl-1* were generated by introducing the
348 *AtSVP* and *CmSVP* gene driven by the 35S promoter, respectively, with molecular
349 identification (Fig. S13). Neither *AtSVP* nor *CmSVP* could revert the phenotype of
350 early flowering that was caused by *tpl-1*, but both *AtSVP* and *CmSVP* overexpression
351 in the WT plants Col-0 delayed flowering significantly (Fig. 6).



352

353 **Fig. 6 Flowering characterization of *AtSVP* and *CmSVP* overexpression plants,**
354 **respectively, in the Col-0 and *tpl-1* background**

355 A. Phenotype of wild type Col-0, *tpl-1*, and transgenic lines in LDs. Scale bar = 1.5
356 cm.

357 B. Statistics of wild type Col-0, *tpl-1*, and transgenic lines in LDs.

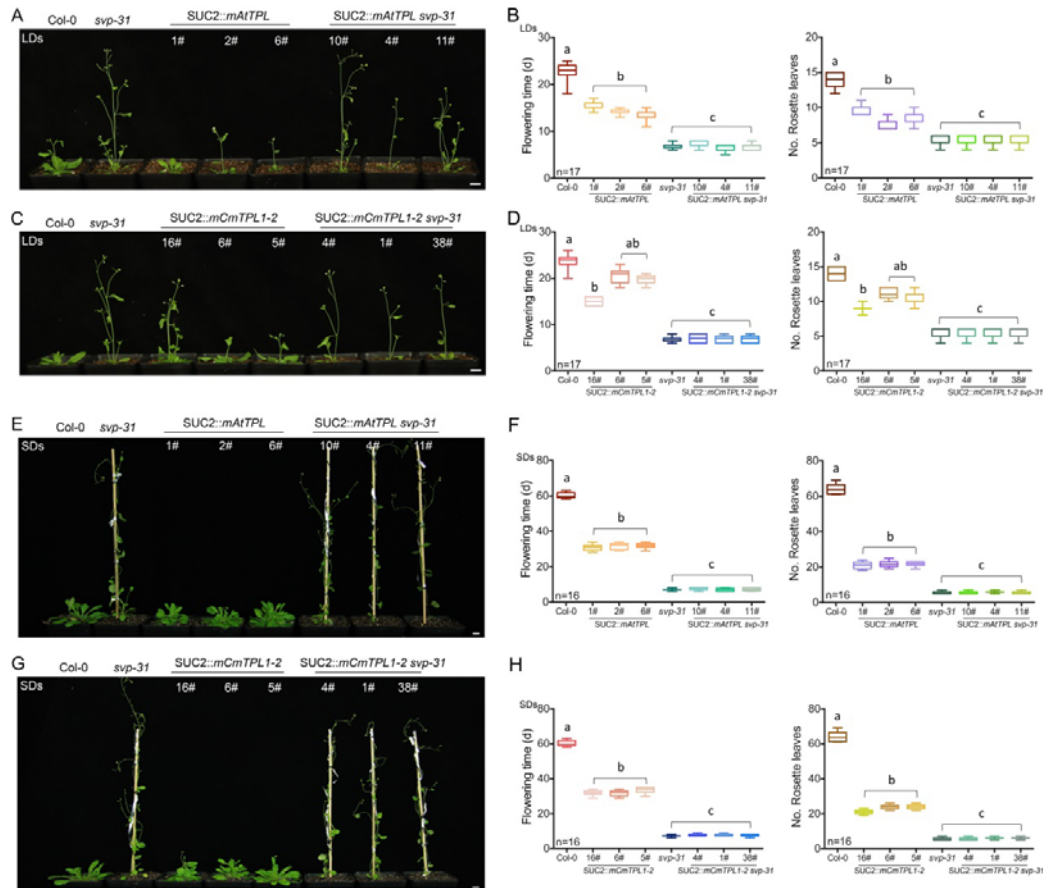
358 C. Phenotypes of wild type Col-0, *tpl-1*, and transgenic lines in SDs. Scale bar = 1.5
359 cm.

360 D. Statistics of wild type Col-0, *tpl-1*, and transgenic lines in SDs.

361 Data represent the mean \pm SEM of biological triplicates. Different letters represent a
362 significant difference at $P < 0.05$ (one-way ANOVA with Fisher's post hoc test).

363 Meanwhile, the late flowering effect of 35S::*CmSVP* and the early flowering effect of
364 35S::*CmSVP-VP64* in *Arabidopsis* reveal that *CmSVP* is a flowering inhibitor; in
365 addition, *CmSVP* was able to fully rescue the *svp-31* mutant of Col-0 (Fig. S11),
366 which genetically suggests that the regulatory function of *CmSVP* in the flowering

367 time of *Arabidopsis* and chrysanthemum is conservative. *FT* is expressed in
368 companion cells of leaf phloem tissues (Chen et al., 2018). To specifically reveal the
369 function of TPL, the construct *SUC2::mAtTPL/SUC2::mCmTPL1-2*
370 (*AtTPL/CmTPL1-2* N176H), which expressed the *tpl-1* mutant protein driven by a
371 *SUCROSE-PROTON SYMPORTER 2* (*SUC2*) phloem companion cell-specific
372 promoter from *Arabidopsis*, was transformed into *Arabidopsis* Col-0 and mutant
373 *svp-31*, respectively, with molecular identification (Fig. S13). We found that the three
374 lines of *SUC2::mAtTPL svp31* (10#, 4#, and 11#) and *SUC2::mCmTPL svp31* (4#, 1#,
375 and 38#) had a similar earlier flowering phenotype with *svp-31* plants either in LDs or
376 SDs compared with the Col-0 WT plants (Fig. 7), which was consistent with that of
377 the double mutant *tpl-1 svp-31*, which had similar early flowering compared with the
378 single mutant (Fig. S12). The molecular identification showed in Fig. S14. These
379 results confirmed that the interaction between TPL and SVP is genetically conserved
380 in *Arabidopsis* and chrysanthemums, and that *SVP* requires TPL/TPR to function as a
381 floral repressor.



382

383 **Fig. 7 Flowering time of SUC::mAtTPL and SUC::mCmTPL1-2 transgenic plants in**
384 **Col-0 and svp-31 backgrounds on long and short days**

385 A and C. Representative images of SUC::mAtTPL/CmTPL1-2/Col-0 and SUC::
386 mAtTPL/CmTPL1-2/svp-31 plants and their parental genetic background (Col-0 and
387 svp-31) under LDs at flowering. Scale bar = 1.5 cm.

388 B and D. Quantification of flowering time (B) and rosette leaf number (D) during
389 long day photoperiods.

390 E and G. Representative images of SUC::mAtTPL/CmTPL1-2/Col-0 and SUC::
391 mAtTPL/CmTPL1-2/svp-31 plants and their parental genetic background (Col-0 and
392 svp-31) under SDs at flowering. Scale bar = 1.5 cm.

393 F and H. Quantification of flowering time (F) and rosette leaf number (H) during
394 short day photoperiods.

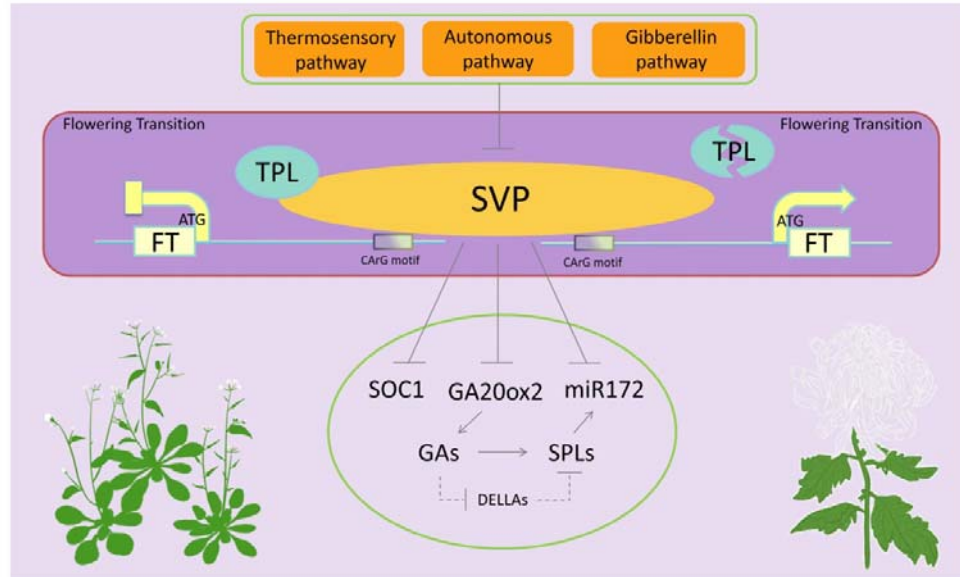
395 Data represent the mean \pm SEM of biological triplicates. Different letters represent a
396 significant difference at $P < 0.05$ (one-way ANOVA with Fisher's post hoc test).

397

398

399 Discussion

400 In this study, the mechanism of SVP in repressing the floral transition in both
401 *Arabidopsis* and chrysanthemums through the interaction with a co-repressor protein
402 TPL was elucidated. There was a conserved EAR motif in SVP proteins which was
403 required for the interaction (Fig. 3), SUC2::*tpl-1* transgenic *Arabidopsis*, or
404 amiR-*CmTPL1-2* transgenic chrysanthemum, attenuates the function of SVP as a
405 transcriptional repressor (Fig. 5,6,7). SVP mediates flowering responses through
406 many pathways, which respond by perceiving signals from different endogenous and
407 environmental factors, such as the GA and thermosensory factors (Gregis et al., 2013;
408 Lee et al., 2013). Recent studies on *Arabidopsis* have demonstrated that GA promotes
409 the expression of *FT* and *SOC1* by suppressing a group of flowering repressors (*ELF3*,
410 *SVP*, *TEM1*, and *TEM2*) via the *GAF1-TPR* complex (Fukazawa et al., 2021). The
411 loss of SVP in *Arabidopsis* suggested that *SVP*-mediated control of the expression of
412 *FT* evolved in the course of the transition from the vegetative to reproductive phase,
413 thus, tracking the changes at the ambient temperature (Lee et al., 2008; Lee et al.,
414 2013; Song et al., 2013). As small non-coding RNAs (microRNAs) act as significant
415 regulatory role during flowering of plants. Studies revealed that miR172 is regulated
416 by SVP and SPL9 (SQUAMOSA PROMOTER BINDING PROTEIN-LIKE 9) of
417 *Arabidopsis* reproduction period (Lee et al., 2010; Zhen et al., 2012). With the gradual
418 in-depth study of SVP homologous genes in plants, the structure and function of SVP
419 have become clearer, but the mechanism of its inhibitory function has not yet been
420 revealed (Gregis et al., 2010; Mauren et al., 2014). Here, the results showed that a
421 SVP-TPL transcriptional complex suppressed *FT* to limit the floral transition during
422 the vegetative phase (Fig. 8).



423

424 **Fig. 8 Schematic representation of SVP and TPL mediating the integration of**
425 **flowering signals.** *SVP* expression is inhibited by the thermosensory, autonomous, and
426 gibberellin (GA) pathways in *Arabidopsis*. Downregulation of *SVP* transcription
427 contributes to increased the expression of *SOC1*, *GA20ox2*, and miR172. Higher GA
428 levels increases the SPLs transcription and release SPLs proteins by DELLAs
429 repression. Arrows and bars indicate promoting and repression effects, respectively.
430 The interactions proposed in this study was shown in the dark purple box with the red
431 outline, *SVP* transcription factor represses a key flowering regulator *FT* by binding to
432 the CARG motif of its promoter both in *Arabidopsis* and chrysanthemum. However,
433 *SVP* need recruit TPL to complete the process of inhibition. In the absence of TPL,
434 the action path of *SVP*-*FT* for flowering will be ineffective.

435

436 *SVP* has a typical plant-specific restriction EAR domain (LXLXLX); however,
437 whether the motif is required for its transcriptional repression activity is unclear (Li et
438 al., 2008; Lisha et al., 2011). For *AtSVP* and *CmSVP*, which were isolated from
439 *Arabidopsis* and chrysanthemums, respectively, the second EAR domain (LRLGLP)
440 of the sequence is essential for interacting with TPL. When it is mutated, the action
441 relationship is invalid and irrelevant to the first EAR domain (Fig. 3). As the

442 conserved EAR motif inhibits transcription processes, the specific function of the first
443 EAR (LELQLV) is unknown.

444 The SVP transcription factor binds to the promoters of *FT*, which completely reverse
445 the effect in triggering an early flowering response(Li et al., 2008). We verified that
446 the process is highly conservative in chrysanthemums (Fig. 2). The two most studied
447 *Arabidopsis* transcriptional repressors for flowering are FLOWERING LOCUS C
448 (FLC) and SVP, which are both present in MADS-box protein(Andrés et al., 2014;
449 Song et al., 2013). FLC can form dimers and function with other redundant
450 MADS-box proteins to suppress flowering by repressing the transcriptions of floral
451 activators, such as *FT* and *SOCI* (Searle et al., 2006). In *Arabidopsis*, the CArG motif
452 (284-302 bp) in the first intron of *FT* can be strongly enriched by FLC proteins, but
453 SVP's binding appears to be weaker than that of FLC (Helliwell et al., 2006; Lee et
454 al., 2007). Studies on SVP have revealed that it is able to bind with the CArG motif
455 (-1235-1225 bp) directly in the *FT* promoter, and this is also the only site on the
456 promoter that exercises the inhibitory function(Lee et al., 2007; Song et al., 2013).
457 This is somewhat different from the site of action in chrysanthemums. Here, we
458 showed, CmSVP was able to target the CArG element in the promoter, 5'UTR, and
459 intron regions, as well as in the promoter. This indicated that the regulation through
460 binding to CArG was conserved.

461 Transcriptional co-repressors play considerable roles in entrenching the adequate
462 levels of gene expression during flowering (Plant et al., 2021). As conserved
463 co-repressors, TPL/TPR was filtered as a partner of SVP in this study. Some previous
464 studies have shown that the floral transition in precise regulation requires TPL/TPR
465 running at multiple points in the pathway to flowering (Espinosa-Ruiz et al., 2017;
466 Fukazawa et al., 2021; Plant et al., 2021; Tao and Estelle, 2018). And moreover, most
467 studies of TPL have been carried out on model plant *Arabidopsis* but not on
468 non-model plants. Here, overexpression of *AtSVP* and *CmSVP* in the *TPL/TPR*
469 loss-of-function mutant *tpl-1* showed futility in delaying flowering (Fig. 6). Moreover,

470 the recruiting dependency relationship between SVP and TPL either in *Arabidopsis* or
471 chrysanthemum was conserved. Experiments in chrysanthemum protoplasts prove the
472 dependence of CmSVP on CmTPL/CmTPR in the process of inhibiting *CmFTL3*
473 transcription (Fig. 5). SVP acts as a core flowering repressor that always functions
474 along with other potent transcription factors (Golembeski and Imaizumi, 2015; Zhen
475 et al., 2012). In *Arabidopsis*, J3 with a typical modular sequence of the J-domain,
476 which encodes a DnaJ-like heat shock protein and often appears as a protein
477 chaperone, represses SVP activity to induce *SOC1* and *FT* expression (Shen et al.,
478 2011; Shen and Yu, 2011). CO interacts with microproteins miP1a/b, TPL, and JM14
479 to prevent flowering in the shoot apical meristem (SAM) until the leaf-derived FT
480 protein triggers the transition to the reproductive growth phase. However, the study
481 did not detect the previously identified TPL/TPR-interacting repression domain
482 containing transcription factors and the formation of a higher order repressor complex
483 is a small process that might be subject to the surrounding conditions (Rodrigues et
484 al., 2021). SVP can interact with TERMINAL FLOWER 2/LIKE
485 HETEROCHROMATIN PROTEIN 1 (TFL2/LHP1) to regulate floral patterning(Liu
486 et al., 2009), while TFL2 recognizes H3K27me3 to repress the expression of many
487 genes including *FT* (Liu et al., 2018). TPL typically associates with histone
488 deacetylase (HDAC) in planta (Krogan et al., 2012), and also interacts with
489 histone-binding protein MSI4, CHROMATIN REMODELLING 4 (Larsson et al.,
490 1998; Turck et al., 2007). This reflects the organizational complexity of flowering
491 transition in plants.

492 As the flowering process in plants is an extremely complex and delicate event and
493 partly accounts for the occurrence of different species and evolutionary adaptation,
494 the crosstalk of SVP with other factors that can ensure the reproductive success
495 remains unknown. Therefore, the interaction between SVP and TPL revealed in this
496 study may represent a rising molecular interconnection among the respective families
497 of conserved regulators, which is linked intermediately to flowering.

498

499 **Materials and Methods**

500 **Plant materials and growing conditions**

501 The experiments were centered on the *C. morifolium* cultivar (cv.) ‘Jinba’, which was
502 obtained from the Chrysanthemum Germplasm Resource Preserving Centre (Nanjing
503 Agricultural University, China). Vegetatively propagated cuttings at the 5–6 leaf stage
504 were grown in a 1:1 mixture of garden soil and vermiculite under a 16 h photoperiod
505 (day/night temperature regime of 23°C/18°C, relative humidity 70%). The
506 *Arabidopsis* plant stocks employed were WT ecotype Col-0 which from The
507 Arabidopsis Information Resource (www.arabidopsis.org/). And the mutants *svp-31*
508 (*SALK_026551*) and *tpl-1* (*At1g15750*) provided respectively by Xu’ lab and He’s lab.
509 All *Arabidopsis* plants were soil-grown under a constant temperature of $22 \pm 2^\circ\text{C}$, a
510 16 h photoperiod, and 70% relative humidity.

511

512 **Isolation and analysis of the gene sequence**

513 Total RNA was extracted using the RNAiso reagent (TaKaRa, Tokyo, Japan) from
514 snap-frozen chrysanthemum leaves of ‘Jinba’, as recommended by the manufacturer.
515 A 1 µg aliquot of RNA was used for the synthesis of the cDNA first strand using a
516 PrimeScriptTMRT reagent Kit containing gDNA eraser (TaKaRa, Shiga, Japan). The
517 cDNA was used as the template and primers in TableS1 were used to PCR amplify the
518 sequence. The amplicon was inserted into the pMD-19T vector (TaKaRa, Tokyo,
519 Japan) by T4 DNA ligase (TaKaRa, Tokyo, Japan) for sequencing. Mutant primers
520 (Table S1) of *CmTPLL1-2* were designed based on the site of the 531 bases (A) to be
521 mutated to C on the website
522 (http://www.bioinformatics.org/primerx/cgi-bin/DNA_3.cgi), which has been
523 described previously (Zhang et al., 2019). The *CmSVP* site was mutated from
524 (TTATTTAAGAAAGCTGAAGAG) to (TTTAAAAAGGCCGAGGAG), which is
525 able to bind miR396(Yang et al., 2015).

526

527 **Transactivation activity assay**

528 LR Clonase™ II enzyme mix (Invitrogen, Carlsbad, CA, USA) was used to
529 recombine with pGBKT7 (Clontech, Mountain View, CA, USA) and pGBKT7-VP16
530 vector (provided by Teng's lab) for the construct. Studies have shown that fusion with
531 VP16 (a fragment of viral DNA sequence encoding the peptide DALDDFDLML) is
532 capable of turning a repressive transcription regulator into an activator (Guo et al.,
533 2018; Suzuki et al., 2014; Triezenberg et al., 1988). A transactivation activity assay
534 was performed following the manufacturer's instructions. Salmon sperm DNA
535 carrying pGBKT7-*CmSVP* (BD-CmSVP), pGBKT7-VP16-CmSVP (VP16-CmSVP),
536 pGBKT7 (BD, negative control), GAL4 and pGBKT7-VP16 (BD-VP16, positive
537 control) inserted into the yeast strain Y2H (Clontech, Mountain View, CA, USA),
538 which next transferred to the SD/-Trp medium. After 3 days, a single clone was
539 selected for cultivating and transferred to the SD/-Trp-His medium with 0 or 20
540 mg/mL X- α -gal. According to the directions, if the protein possesses transcriptional
541 activation activity, it should bind to the GAL4-BD upstream promoter sequence of
542 *His3* as the GAL4-BD could regulate the *His3* expression. As a result, yeast colonies
543 grew on SD/-Trp-His and turned blue on SD/-Trp-His with X- α -gal.

544

545 **Subcellular localization**

546 The full-length coding region (minus the termination codon) was amplified with
547 appropriate modifications, generating 35S::GFP-CmSVP. It was then transformed into
548 protoplasts of wild-type 'Jinba' after incubation for 12–14 h at 28°C. GFP
549 fluorescence was then detected using a confocal laser scanning microscope (LSM800,
550 Zeiss).

551

552 **Yeast two-hybrid assay**

553 The coding regions of *CmTPL1-2* was amplified and cloned into pGADT7, and

554 *CmSVP* or *CmSVP*-mut1/mut2 was amplified and cloned into pGBKT7 (Clontech) for
555 Y2H assays. The Yeastmaker Yeast Transformation System 2 was used according to
556 the manufacturer's instructions (Clontech). pGBK-53 and pGADT were used as
557 positive controls, while pGBK-Lam and pGADT were used as negative controls. All
558 combinations were transferred to the SD/-Leu-Trp medium by the yeast strain Y2H
559 (Clontech, Mountain View, CA, USA), and then transferred to the SD/-Leu-Trp
560 medium. Yeast colonies were grown on SD/-Leu-Trp-His-Ade and turned blue on
561 SD/-Leu-Trp-His-Ade containing X- α -gal if an interaction existed between the
562 proteins.

563

564 **RNA isolation and gene expression analysis**

565 Samples were taken when the transgenic material and WT were grown till 18–20
566 leaves appeared under LD conditions (16 h/8 h photoperiod) and then transferred to
567 SD conditions (8 h/16 h photoperiod) for 3 days. Meanwhile, SAM and mature leaves
568 were selected, and samples were taken in the early morning (*FT* gene expression was
569 the highest). Quantitative primer of *CmFTL3* is designed according to the sequence
570 provided by <http://172.30.0.105/VIROBLAST/VIROBLAST>. PHP sequence design
571 The cDNA was used as the template for qRT-PCRs based on Fast SYBR Green
572 Master Mix (www.bimake.com). The qRT-PCR involved an initial denaturation
573 (95°C/2 min), followed by 40 cycles of 95°C/15 s, 60°C/15 s, and 72°C/15 s. The
574 reference sequence was the *Actin8* gene for *Arabidopsis* and *C. nankingense EF1 α*
575 gene for chrysanthemums, and the relative transcript abundances were calculated
576 using the $2^{-\Delta\Delta CT}$ method (Livak and Schmittgen, 2001). The set of qRT-PCR primer
577 sequences used is listed in Table S3.

578

579 ***Arabidopsis* transformation**

580 The p35S::*CmSVP*, p35S::*AtSVP*, 35S::*CmSVP-VP64*, p35S::*CmTPL1-2*,
581 p35S::*AtTPL1-2*, SUC2::*mCmTPL1-2* and SUC2::*mAtTPL1-2* transgenes were

582 introduced into *Arabidopsis* by the *A. tumefaciens* strain EHA105. 1/2 of the MS
583 medium, which contained 50 $\mu\text{g mL}^{-1}$ hygromycin or 1 $\mu\text{g mL}^{-1}$ kanamycin, was
584 applied for transformed progeny selection. Each of three independent T3 transgenic
585 plants was obtained and validated by using the PCR primer pair in Table S1 and S2
586 for amplification.

587

588 **Co-immunoprecipitation assay**

589 Co-IP assays were conducted at He's Laboratory (Li et al., 2018). Briefly, the total
590 protein was extracted from tobacco expressing CmTPL1-2-HA and CmSVP-FLAG
591 using anti-HA affinity gel (E6779, Sigma), followed by western blotting with
592 anti-FLAG (A8592, Sigma), and anti-HA (12013819001, Roche).

593

594 **Yeast one-hybrid assay**

595 The CDSs of CmSVP were inserted into the pGADT7 vector to generate the
596 recombinant construct pGADT7-CmSVP, while the CDS of GUS (β -glucuronidase)
597 was inserted into the pGADT7 vector as the negative control. The *CmFTL3* promoter
598 and 5'UTR fragments were cloned into the pHis2 vector. The primer pairs used for
599 gene cloning are listed in Supplementary Table S1. Subsequently, all constructs were
600 transformed into *Saccharomyces cerevisiae* strain Y187 using the lithium acetate
601 method. Subsequently, yeast cells were inoculated on a selective medium lacking Trp,
602 Leu, and His (SD/-Trp/-Leu/-His). The selected colonies were then inoculated on a
603 -Trp/-Leu/-His medium supplemented with an appropriate concentration of 3-AT and
604 grown for 3 days at 28°C, the binding was identified by spot assay.

605

606 **Dual-luciferase reporter assay (leaves of *N. benthamiana*)**

607 The fragment of the *CmFTL3* promoter (<http://172.30.0.105/viroblast/viroblast.php>)
608 was cloned into the pGreenII0800-Luc vector, which contained a reporter gene
609 encoding firefly luciferase (kindly provided by Dr. Huazhong Shi, Texas Tech

610 University, Lubbock, TX). *A. tumefaciens* strain GV3101 harboring *CmFTL3::LUC*,
611 *p35S::GFP-CmSVP*, *p35S::GFP-CmTPL1-2*, and *p35S::GFP* was grown in infiltration
612 medium (2 mM Na₃PO₄, 50 mM MES, 100 mM acetosyringone) to an OD₆₀₀ of 0.5
613 and then introduced via a syringe into the leaf of a 4–5-week-old *Nicotiana*
614 *benthamiana* plant. After 48–96 h, a CCD camera was used to observe luciferase
615 activity.

616

617 **Dual-luciferase reporter assay (protoplasts of chrysanthemums)**

618 Overall, 10 µg plasmid of *proCmFTL3-P1*, *35S::CmSVP-Flag*, *35S::CmTPL1-2-Flag*,
619 and *35S::Flag* were transformed to *amiR-CmTPL1-2* and *35S::CmTPL1-2* (heat shock
620 induced vector, pMDC30) transgenic lines of chrysanthemum protoplasts. After 40%
621 PEG-mediated transformation, the protoplasts were placed in a dark environment at
622 24°C for 20 h. It should be emphasized that *35S::CmTPL1-2* (heat shock induced
623 vector, pMDC30) can be expressed only after treatment with 37°C, and wild-type
624 ‘Jinba’ of chrysanthemum was used as the control. The Renilla and firefly luciferase
625 activities were measured using a Dual-luciferase Reporter Assay System (Promega,
626 cat. # e1910).

627

628 **Electrophoretic mobility shift assay (EMSA)**

629 The fusion proteins of CmSVP were generated through prokaryotic expression in vitro.
630 The CDSs of CmSVP were cloned into the PGEX-5T vector containing a Gst (GST)
631 target to generate recombined vectors. Then, these recombined vectors were
632 transformed into *Escherichia coli* BL21 (DE3). IPTG was used to induce protein
633 production. The fusion proteins were purified using the MagneGST™ Pull-Down
634 System (Promega). The subsequent EMSAs were performed using a LightShift™
635 Chemiluminescent EMSA Kit (Thermo Fisher, New York), following the
636 manufacturer’s instructions. The GST protein was used as a negative control, and
637 unlabeled probes were used for probe competition. The resulting samples were loaded

638 onto a pre-run native 6.5% polyacrylamide gel using TBE buffer as the electrolyte.
639 After electro-blotting onto a nylon membrane (Millipore, Darmstadt, Germany) and
640 UV cross-linking (2000 J for 5 min), the membrane was incubated in blocking buffer
641 for 30 min and rinsed in washing buffer. Finally, a CCD camera was used to visualize
642 the chemiluminescent signal.

643

644 **ChIP-qPCR assay**

645 The transgenic chrysanthemum p35S::GFP-*CmSVP* was applied to the ChIP-qPCR
646 assays. Moreover, the EpiTect ChIP OneDay Kit (Qiagen) was used according to the
647 manufacturer's instructions. A GFP-specific antibody was used in the assay.
648 Subsequent quantitative real-time PCR (qRT-PCR) used sequence-specific primers,
649 which are provided in Table S3.

650

651 **Acknowledgements**

652 This work was financially supported grants from the National Natural Science
653 Foundation of China (31872146), and a project funded by the Priority Academic
654 Program Development of Jiangsu Higher Education Institutions. We thank Dr.
655 Yuehua Ma (Central laboratory of College of Horticulture, Nanjing Agricultural
656 University) for assistance in using ultra high resolution confocal microscope
657 (LSM800, Zeiss, Germany).

658

659 **Author contributions**

660 J.F.J., F.D.C, and Z.X.Z. conceived and designed the experiments; Z.X.Z., H.Q. and
661 Y. Q.Z. performed most of the experiments; G.Z., E.L.S, G.F.L, W.X.L and X.R.C.
662 provided technical support; Y.H.H, S.B., S.M.C, W.M.F. and Z.Y.G. provided
663 conceptual advice; G.Z., H.Q. and Z.X.Z. contributed to the Co-IP assay; E.L.S. and
664 H.Q. contributed to the ChIP assay; H.Q., Z.X.Z., Y.Q.Z. and R.Q.H contributed to

665 plants transformation; Z.X.Z., H.Q. and J.F.J. analyzed the data and wrote the
666 manuscript.

667

668 **Conflicts of interest**

669 The authors declare that they have no conflicts of interest.

670

671

Parsed Citations

- Andrés, F., Porri, A., Torti, S., Mateos, J., Romera-Branchat, M., García-Flores, L., Martin-Magniette, M. L., and Coupland, G. (2014). SHORT VEGETATIVE PHASE reduces gibberellin biosynthesis at the Arabidopsis shoot apex to regulate the floral transition. *PNAS* 111, E2760-E2769.
Google Scholar: [Author Only](#) [Title Only](#) [Author and Title](#)
- Causier, B., Ashworth, M., Guo, W. J., and Davies, B. (2012). The TOPLESS interactome: a framework for gene repression in Arabidopsis. *Plant physiol.* 158, 423-38.
Google Scholar: [Author Only](#) [Title Only](#) [Author and Title](#)
- Chen, Q., Payyavula, R., Lin, C., Jing, Z., and Turgeon, R. (2018). FLOWERING LOCUS T mRNA is synthesized in specialized companion cells in Arabidopsis and Maryland Mammoth tobacco leaf veins. *PNAS* 115, 2830-2835.
Google Scholar: [Author Only](#) [Title Only](#) [Author and Title](#)
- Cheng, P., Wang, D., Cao, P., Liu, Y., and Gao, J. (2018). A Transcriptomic Analysis Targeting Genes Involved in the Floral Transition of Winter-Flowering Chrysanthemum. *J Plant Growth Regul.* 37(1), 220-232.
Google Scholar: [Author Only](#) [Title Only](#) [Author and Title](#)
- Espinosa-Ruiz, A., Martínez, C., Lucas, M. D., Fàbregas, N., Bosch, N., Caño-Delgado, A. I., and Prat, S. (2017). TOPLESS mediates brassinosteroid control of shoot boundaries and root meristem development in Arabidopsis thaliana. *Dev.* 144, 1619-1628.
Google Scholar: [Author Only](#) [Title Only](#) [Author and Title](#)
- Fernández, V., Takahashi, Y., Gourrierc, J. L., and Coupland, G. (2016). Photoperiodic and thermosensory pathways interact through CONSTANS to promote flowering at high temperature under short days. *Plant J.* 86.
Google Scholar: [Author Only](#) [Title Only](#) [Author and Title](#)
- Folter, S., and Angenent, G. (2006). trans meets cis in MADS science. *Trends Plant Sci.* 11, 224-231.
Google Scholar: [Author Only](#) [Title Only](#) [Author and Title](#)
- Fukazawa, J., Ohashi, Y., Takahashi, R., Nakai, K., and Takahashi, Y. (2021). DELLA degradation by gibberellin promotes flowering via GAF1-TPR-dependent repression of floral repressors in Arabidopsis. *Plant Cell* 33, 2258-2272.
Google Scholar: [Author Only](#) [Title Only](#) [Author and Title](#)
- Golembeski, G., and Imaizumi, T. (2015). Photoperiodic Regulation of Florigen Function in Arabidopsis thaliana. *Arabidopsis Book* 13, e0178.
Google Scholar: [Author Only](#) [Title Only](#) [Author and Title](#)
- Goraloglia, G., Liu, T., Zhao, L., Panipinto, P., Groover, E., Bains, Y., and Imaizumi, T. (2017). CYCLING DOF FACTOR 1 represses transcription through the TOPLESS co-repressor to control photoperiodic flowering in Arabidopsis. *Plant J.* 92, 244-262.
Google Scholar: [Author Only](#) [Title Only](#) [Author and Title](#)
- Graeff, M., Straub, D., Eguen, T., Dolde, U., and Rodrigues, V. (2016). MicroProtein-Mediated Recruitment of CONSTANS into a TOPLESS Trimeric Complex Represses Flowering in Arabidopsis. *Plos Genet.* 12, e1005959.
Google Scholar: [Author Only](#) [Title Only](#) [Author and Title](#)
- Gregis, V., Andrés, F., Sessa, A., and Guerra, R. F. (2013). Identification of pathways directly regulated by SHORT VEGETATIVE PHASE during vegetative and reproductive development in Arabidopsis. *Genome Biol.* 14, R56.
Google Scholar: [Author Only](#) [Title Only](#) [Author and Title](#)
- Gregis, V., Sessa, A., Colombo, L., and Kater, M. M. (2010). AGAMOUS-LIKE24 and SHORT VEGETATIVE PHASE determine floral meristem identity in Arabidopsis. *Plant J.* 56, 891-902.
Google Scholar: [Author Only](#) [Title Only](#) [Author and Title](#)
- Guo, S., Dai, S., Singh, P. K., Wang, H., Wang, Y., Tan, J., Wanyi, W., and Toshiro, I. (2018). A Membrane-Bound NAC-Like Transcription Factor OsNTL5 Represses the Flowering in Oryza sativa. *Frontiers in Plant Science* 9, 555.
Google Scholar: [Author Only](#) [Title Only](#) [Author and Title](#)
- Hartmann, U., Hhmann, S., Nettesheim, K., Wisman, E., Saedler, H., and uijser, P. H. (2000). Molecular cloning of SVP: a negative regulator of the floral transition in Arabidopsis. *Plant J.* 21.
Google Scholar: [Author Only](#) [Title Only](#) [Author and Title](#)
- Hartmann, U., Höhmann, S., Nettesheim, K., Wisman, E., and Huijser, P. (2010). Molecular cloning of SVP: a negative regulator of the floral transition in Arabidopsis. *Plant J.* 21, 351-360.
Google Scholar: [Author Only](#) [Title Only](#) [Author and Title](#)
- Helliwell, C., Wood, C., Robertson, M., Peacock, W., and Dennis, E. (2006). The Arabidopsis FLC protein interacts directly in vivo with SOC1 and FT chromatin and is part of a high-molecular-weight protein complex. *Plant J.* 46, 183-192.
Google Scholar: [Author Only](#) [Title Only](#) [Author and Title](#)
- Higuchi, Y., Narumi, T., Oda, A., Nakano, Y., Sumitomo, K., Fukai, S., and Hisamatsu, T. (2013). The gated induction system of a systemic floral inhibitor, antiflorigen, determines obligate short-day flowering in chrysanthemums. *PNAS* 110, 17137-17142.
Google Scholar: [Author Only](#) [Title Only](#) [Author and Title](#)

- Jang, S., Torti, S., and Coupland, G. (2009). Genetic and spatial interactions between FT, TSF and SVP during the early stages of floral induction in *Arabidopsis*. *Plant J.* 60.
Google Scholar: [Author Only](#) [Title Only](#) [Author and Title](#)
- Kinoshita, A., and Richter, R. (2020). Genetic and molecular basis of floral induction in *Arabidopsis thaliana*. *J. Exp. Bot.* 71, 2490-2504.
Google Scholar: [Author Only](#) [Title Only](#) [Author and Title](#)
- Krogan, N., Hogan, K., and Long, J. (2012). APETALA2 negatively regulates multiple floral organ identity genes in *Arabidopsis* by recruiting the co-repressor TOPLESS and the histone deacetylase HDA19. *Dev.* 139, 4180-90.
Google Scholar: [Author Only](#) [Title Only](#) [Author and Title](#)
- Larsson, A., Landberg, K., and Meeks-Wagner, D. (1998). The TERMINAL FLOWER2 (TFL2) gene controls the reproductive transition and meristem identity in *Arabidopsis thaliana*. *Genet.* 149, 597-605.
Google Scholar: [Author Only](#) [Title Only](#) [Author and Title](#)
- Lee, H., Yoo, S., Lee, J., Kim, W., and al., e. (2010). Genetic framework for flowering-time regulation by ambient temperature-responsive miRNAs in *Arabidopsis*. *Nucleic Acids Res.* 38, 3081-3093.
Google Scholar: [Author Only](#) [Title Only](#) [Author and Title](#)
- Lee, J., Lee, J., and Ji, H. (2008). Ambient temperature signaling in plants: An emerging field in the regulation of flowering time. *J Plant Biol.* 51, 321-326.
Google Scholar: [Author Only](#) [Title Only](#) [Author and Title](#)
- Lee, J., Ryu, H., Chung, K., Pose, D., Kim, S., Schmid, M., and Ann, J. (2013). Regulation of Temperature-Responsive Flowering by MADS-Box Transcription Factor Repressors. *Science* 342, 628-632.
Google Scholar: [Author Only](#) [Title Only](#) [Author and Title](#)
- Lee, J., Yoo, S., Park, S., Hwang, I., Lee, J., and Ahn, J. (2007). Role of SVP in the control of flowering time by ambient temperature in *Arabidopsis*. *Genes Dev* 21, 397-402.
Google Scholar: [Author Only](#) [Title Only](#) [Author and Title](#)
- Leydon, A., Wang, W., Gala, H., Gilmour, S., and Nemhauser, J. (2021). Repression by the *Arabidopsis* TOPLESS corepressor requires association with the core mediator complex. *eLife* 10, e66739.
Google Scholar: [Author Only](#) [Title Only](#) [Author and Title](#)
- Li, D., Chang, L., Shen, L., Yang, W., Chen, H., Robertson, M., Helliwell, C. A., Ito, T., Meyerowitz, E., and Hao, Y. (2008). A Repressor Complex Governs the Integration of Flowering Signals in *Arabidopsis*. *Dev. Cell* 15, 110-120.
Google Scholar: [Author Only](#) [Title Only](#) [Author and Title](#)
- Li, Z., Jiang, D., and He, Y. (2018). FRIGIDA establishes a local chromosomal environment for FLOWERING LOCUS C mRNA production. *Nat. Plants* 4, 836-846.
Google Scholar: [Author Only](#) [Title Only](#) [Author and Title](#)
- Lisha, S., Germain, K., Lu, L., and Hao, Y. (2011). The J-domain protein J3 mediates the integration of flowering signals in *Arabidopsis*. *Plant Cell* 23, 499-514.
Google Scholar: [Author Only](#) [Title Only](#) [Author and Title](#)
- Liu, C., Xi, W., Shen, L., Tan, C., and Hao, Y. (2009). Regulation of floral patterning by flowering time genes. *Dev. Cell* 16, 711-722.
Google Scholar: [Author Only](#) [Title Only](#) [Author and Title](#)
- Liu, X., Sun, Z., Dong, W., Wang, Z., and Zhang, L. (2018). Expansion and Functional Divergence of the SHORT VEGETATIVE PHASE (SVP) Genes in Eudicots. *Genome Biol. Evol.* 10, 3026-3037.
Google Scholar: [Author Only](#) [Title Only](#) [Author and Title](#)
- Livak, K., and Schmittgen, T. (2001). Analysis of Relative Gene Expression Data Using Real-Time Quantitative PCR and the $2^{-\Delta\Delta C T}$ Method. *Methods* 25, 402-408.
Google Scholar: [Author Only](#) [Title Only](#) [Author and Title](#)
- Long, J., Ohno, C., Smith, Z., and Meyerowitz, E. (2006). TOPLESS Regulates Apical Embryonic Fate in *Arabidopsis*. *Science* 312, 1520-1523.
Google Scholar: [Author Only](#) [Title Only](#) [Author and Title](#)
- Mauren, J., Jacob, M., Zhang, L., Wen, J., Mysore, K., Richard, M., and Joanna, P. (2014). Overexpression of *Medicago* SVP genes causes floral defects and delayed flowering in *Arabidopsis* but only affects floral development in *Medicago*. *J Exp Bot.* 65, 429-442.
Google Scholar: [Author Only](#) [Title Only](#) [Author and Title](#)
- Oda, A., Narumi, T., Li, T., Kando, T., Higuchi, Y., Sumitomo, K., Fukai, S., and Hisamatsu, T. (2012). CsFTL3, a chrysanthemum FLOWERING LOCUS T-like gene, is a key regulator of photoperiodic flowering in chrysanthemums. *J. Exp. Bot.* 63, 1461-1477.
Google Scholar: [Author Only](#) [Title Only](#) [Author and Title](#)
- Palatnik, J., Allen, E., Wu, X., Schommer, C., and Schwab, R. (2003). Control of leaf morphogenesis by microRNAs. *Nature* 425, 257-263.
Google Scholar: [Author Only](#) [Title Only](#) [Author and Title](#)

Pauwels, L., Barbero, G. F., G Ee Rinck, J., Tilleman, S., Grunewald, W., Pérez, A., Chico, J. M., Bossche, R. V., Sewell, J., and Gil, E. (2010). NINJA connects the co-repressor TOPLESS to jasmonate signalling. *Nature* 464, 788-91.

Google Scholar: [Author Only Title Only Author and Title](#)

Plant, A, Larrieu, A, and Casuier, B. (2021). Repressor for hire! The vital roles of TOPLESS-mediated transcriptional repression in plants. *New Phytol.* 231, 963-973.

Google Scholar: [Author Only Title Only Author and Title](#)

Rodrigues, V., Dolde, U., Sun, B., Blaakmeer, A, Straub, D., Eguen, T., Botterweg-Paredes, E., Hong, S., Graeff, M., Li, M.-W., Gendron, J. M., and Wenkel, S. (2021). A microProtein repressor complex in the shoot meristem controls the transition to flowering. *Plant Physiol.* 187, 187-202.

Google Scholar: [Author Only Title Only Author and Title](#)

Searle, I., Vincent, C., Coupland, G., Amasino, R. A, He, Y., Turck, F., Fornara, F., and Krober, S. (2006). The transcription factor FLC confers a flowering response to vernalization by repressing meristem competence and systemic signaling in *Arabidopsis*. *Gene Dev.* 20, 898-912.

Google Scholar: [Author Only Title Only Author and Title](#)

Shen, L., Germain, K. G., Lu, L., and Yu, H. (2011). The J-domain protein J3 mediates the integration of flowering signals in *Arabidopsis*. *Plant Cell* 23, 499-514.

Google Scholar: [Author Only Title Only Author and Title](#)

Shen, L., and Yu, H. (2011). J3 regulation of flowering time is mainly contributed by its activity in leaves. *Plant Signal Behav.* 6, 601-603.

Google Scholar: [Author Only Title Only Author and Title](#)

Song, Y., Ito, S., and Imaizumi, T. (2013). Flowering time regulation: photoperiod- and temperature-sensing in leaves. *Trends Plant Sci.* 18, 575-583.

Google Scholar: [Author Only Title Only Author and Title](#)

Suzuki, Ohme-Takagi, Kigoshi, Sakamoto, and Fujiwara (2014). VP16 fusion induces the multiple-knockout phenotype of redundant transcriptional repressors partly by Med25-independent mechanisms in *Arabidopsis*. *FEBS Letters* 588, 3665-3672.

Google Scholar: [Author Only Title Only Author and Title](#)

Szemenyei, H., Hannon, M., and Long, J. (2008). TOPLESS Mediates Auxin-Dependent Transcriptional Repression During *Arabidopsis* Embryogenesis. *Science* 319, 1384-1386.

Google Scholar: [Author Only Title Only Author and Title](#)

Tao, S., and Estelle, M. (2018). Mutational studies of the Aux/IAA proteins in *Physcomitrella* reveal novel insights into their function. *New Phytol.* 218, 1534-1542.

Google Scholar: [Author Only Title Only Author and Title](#)

Teixeira, J. (2003). *Chrysanthemum*: advances in tissue culture, cryopreservation, postharvest technology, genetics and transgenic biotechnology. *Biotechnol Adv.* 21, 715-766.

Google Scholar: [Author Only Title Only Author and Title](#)

Triezenberg, S. J., Kingsbury, R. C., and Mcknight, S. L. (1988). Functional dissection of VP16, the trans-activator of herpes simplex virus immediate early gene expression. *Genes & Development* 2, 718-29.

Google Scholar: [Author Only Title Only Author and Title](#)

Turck, F., Roudier, F., Farrona, S., Martin-Magniette, M. L., and Colot, V. (2007). *Arabidopsis* TFL2/LHP1 Specifically Associates with Genes Marked by Trimethylation of Histone H3 Lysine 27. *PLoS Genet.* 3, 0855-0866.

Google Scholar: [Author Only Title Only Author and Title](#)

Wang, L., Sun, J., Ren, L., Zhou, M., and Jiang, J. (2020). CmBBX8 accelerates flowering by targeting CmFTL1 directly in summer chrysanthemum. *Plant Biotechnol J.* 18, 1-11.

Google Scholar: [Author Only Title Only Author and Title](#)

Wei, Y., Wang, T., Chen, Y., Zhang, L., and Jiang, C. (2017). Control of chrysanthemum flowering through integration with an aging pathway. *Nat Commun.* 8, 1-11.

Google Scholar: [Author Only Title Only Author and Title](#)

Yang, C., Huang, Y.-H., Lin, C.-P., Lin, Y.-Y., Hsu, H.-C., Wang, C.-N., Liu, L.-Y. D., Shen, B.-N., and Lin, S.-S. (2015). MicroRNA396-Targeted SHORT VEGETATIVE PHASE Is Required to Repress Flowering and Is Related to the Development of Abnormal Flower Symptoms by the Phyllody Symptoms1 Effector. *Plant Physiol.* 168, 1702-1716.

Google Scholar: [Author Only Title Only Author and Title](#)

Yang, Y., Ma, C., Xu, Y., Wei, Q., Imtiaz, M., Lan, H., Gao, S., Cheng, L., Wang, M., and Fei, Z. (2014). A Zinc Finger Protein Regulates Flowering Time and Abiotic Stress Tolerance in *Chrysanthemum* by Modulating Gibberellin Biosynthesis. *Plant Cell* 26, 2038-2054.

Google Scholar: [Author Only Title Only Author and Title](#)

Zhang, Z., Hu, Q., Cheng, H., Cheng, P., Liu, Y., Liu, W., Xing, X., Chen, S., Chen, F., and Jiang, J. (2019). A single residue change in the product of the chrysanthemum gene TPL1-2 leads to a failure in its repression of flowering. *Plant Sci.* 285, 165-174.

Google Scholar: [Author Only Title Only Author and Title](#)

Zhen, T., Shen, L., Chang, L., Lu, L., Yan, Y., and Yu, H. (2012). Genome-wide identification of SOC1 and SVP targets during the floral transition in Arabidopsis. Plant J. 70, 549-561.

Google Scholar: [Author Only](#) [Title Only](#) [Author and Title](#)